IUTAM Symposium on *Critical flow dynamics involving moving/deformable structures with design applications*, June 18-22, 2018, Santorini, Greece

NUMERICAL SIMULATION ON A FIXED MESH FOR THE FEEDBACK STABILIZATION OF A FLUID–STRUCTURE INTERACTION SYSTEM WITH A STRUCTURE GIVEN BY A FINITE NUMBER OF PARAMETERS

G. Delay*, S. Ervedoza*, M. Fournié* and G. Haine**

* Institut de Mathématiques, UMR 5219 Université Paul Sabatier, CNRS, Toulouse

** Institut Supérieur de l'Aéronautique et de l'Espace, Toulouse, France

Email : guillaume.delay@math.univ-toulouse.fr, sylvain.ervedoza@–, michel.fournie@– and ghislain.haine@isae.fr

Abstract.

We study the numerical approximation of a 2d fluid–structure interaction problem stabilizing the fluid flow around an unstable stationary solution in presence of boundary perturbations. The structure is governed by a finite number of parameters and a feedback control law acts on their accelerations. The existence of strong solutions and the stabilization of this fluid–structure system were recently studied in [3]. The present work is dedicated to the numerical simulation of the problem using a fictitious domain method based on extended Finite Element [4]. The originality of the present work is to propose efficient numerical tools that can be extended in a simple manner to any fluid-structure control simulation. Numerical tests are given and the stabilization at an exponential decay rate is observed for small enough initial perturbations.

Key words: fluid-structure interaction, DNS, fictitious domain, XFEM, control, incompressible flow.

1 Introduction

Critical flow dynamics involving moving/deformable structures with design applications has been receiving increasing attention from the scientific community. In the context of aeronautics, control flow by morphing remains a challenge [7] as well on a comprehensive study of the physical problems as on a development of robust numerical methods [9].

1.1 Position of the problem

The question of how to design moving/deformable structures to control flow requires a rigorous justification of the process corresponding to study the following concepts.

- The modeling of the 2d fluid–structure model. In the present work, we consider a structure described by a finite number of parameters with a feedback control law acting on the acceleration of the structure, see [3].
- The well–posedness of the system. We refer to [3] for the proof of the existence and uniqueness of strong solution.
- The stabilizability of the continuous fluid–structure system. Under a unique continuation assumption for the eigenvectors of the adjoint system, a nonlinear feedback

control is proposed to stabilize the whole fluid–structure system around a stationary solution at any chosen exponential decay rate for small enough initial perturbations, see [3]. The method reposes on the analysis of the linearized system and the feedback operator is given by a Riccati equation of small dimension (Reduced Order Model). This feedback control is able to stabilize the nonlinear semi-discrete controlled system.

- The semi-discretization in space of the infinite dimensional system. The stabilization of such a system must be studied even if the strategy is the same as the one used for the continuous problem. The justification is not straightforward and requires a specific proof for each new fluid–structure system. The numerical method retained for the discretization is the finite element method that can be used for complex geometry.
- The time evolution and numerical simulations. Beyond the well-known difficulties encountered to consider fluid–structure interactions to match the motion of the structure into the fluid (time evolution of the computational domain) [9], the contribution of the control control requires a specific attention.

1.2 Previous work

The continuous problem has already been studied in [3] and a similar approach to ours has been investigated in [8]. Other similar studies have already been led for the Navier–Stokes equations [1] and for a fluid–structure interaction problem [10]. This latter work is based on computations that are formulated into a fixed domain after a change of variables. However this mapping introduces nonlinear terms that are difficult to implement (introducing numerical errors) and involves a high computational time. In opposite, in the present work all computations are done in the time dependent fluid domain. Preparatory work relating to this was done in a simpler situation where the control is governed by the fluid only and the deformation of the structure is located on small parts of its boundary [5]. This difficulty is addressed using a fictitious domain approach based on an extended finite element method. More precisely, the focus is on the so-called geometrically unfitted finite element methods where the solution of the PDE typically remains a standard finite element method, but the variational formulation is modified so that the constraints on the interface and boundaries can be integrated in the computation even if the mesh is not fitted to the geometry. In such approaches, the computational mesh used is independent of the physical domain. These methods are called CutFEM and can be viewed as particular XFEM methods, see [4].

1.3 Outline

The outline of the paper is as follows. In Section 2, we present the setting of the problem that can be extended to more general system and we introduce the diffeomorphism that allows to model the deformation of the structure. In Section 3, we recall the principles to construct a feedback control law for the linear problem and give the synopsis of these ideas. In Section 4, the discretization of the fluid–structure system based on fictitious domain method is introduced before the presentation of the time evolution partitioned algorithm. Finally, in Section 5, numerical simulations with original treatment of the control are reported. We compare the results obtained with and without applying the control to the nonlinear fluid–structure system.

2 Setting of the problem and modelling of the deformation

2.1 The fluid–structure model

The global domain represents a wind tunnel $\Omega \subset \mathbb{R}^2 = (0, L)\times(0, 1)$. Dirichlet boundary conditions are imposed on $\Gamma_i = \{0\} \times (0, 1)$ the inflow region, on $\Gamma_w = (0, L) \times \{0, 1\}$ the upper and lower walls ($\Gamma_D = \Gamma_i \cup \Gamma_w$) and Neumann conditions are retained on $\Gamma_{\rm N} = \{L\} \times (0, 1)$ the outflow region. We use a smooth approximation of a steering gear structure $S(\theta_1(t), \theta_2(t))$ depending on two parameters and the fluid fills the time evolving domain $\mathscr{F}(\theta_1(t), \theta_2(t)) = \Omega\backslash S(\theta_1(t), \theta_2(t))$.
Note that the structure can be viewed like an assembling of one solid S_1 tied to the fixed frame by a pivoting link O and an other solid S_2 tied to solid S_1 by a pivoting link P. S_1 can be thought of as the aerofoil of a wing and S_2 as a steering gear such as an aileron.
The deformation of the structure is linked to its reference configuration $S_{\rm ref}$ by a smooth diffeomorphism $\mathbf{X}(\theta_1, \theta_2, .)$ and we denote $\mathbf{Y}(\theta_1, \theta_2, .)$ its inverse, see Fig.1.

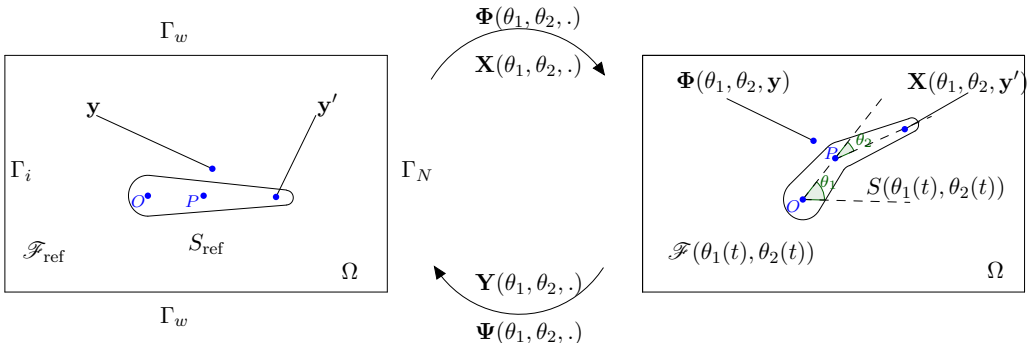

Figure 1: Real and reference structure configurations.

The fluid is modeled by the incompressible Navier-Stokes equations. The equations of the structure are derived from a virtual work principle.

$$\left\{\begin{array}{l} \text{Find } (\theta_1(t),\theta_2(t)) \in \mathbb{D}_\Theta, \text{ such that } \forall \mathbf{w} \in \mathrm{Vect}(\partial_{\theta_1}\mathbf{X}(\theta_1(t),\theta_2(t),.), \partial_{\theta_2}\mathbf{X}(\theta_1(t),\theta_2(t),.)), \\ \displaystyle\int_{S_{\rm ref}} \rho \frac{\mathrm{d}^2}{\mathrm{d}t^2}(\mathbf{X}(\theta_1(t),\theta_2(t),\mathbf{y}))\cdot\mathbf{w}(\mathbf{y})\mathrm{d}\mathbf{y} + \int_{\partial S(\theta_1(t),\theta_2(t))} \sigma_F(\mathbf{u},p)\mathbf{n}_{\theta_1,\theta_2}\cdot\mathbf{w}(\mathbf{Y}(\theta_1(t),\theta_2(t),\gamma_x))\mathrm{d}\gamma_x = 0, \end{array}\right.$$

where $\rho > 0$ is a constant modeling the mass per unit volume, $\mathbf{n}_{\theta_1,\theta_2}$ is the outward unitary normal to the fluid domain and $\sigma_F(\mathbf{u}, p) = -p\mathrm{I} + \nu(\nabla\mathbf{u} + \nabla\mathbf{u}^T)$, where ν is the viscosity of the fluid and $\mathbb{D}_\Theta$ is an admissible domain which is an open connected subset of $\mathbb{R}^2$. We denote $\mathbf{n}$ and $\mathbf{n}_{\theta_1,\theta_2}$ the outward unitary normals to Ω and to $\mathscr{F}(\theta_1(t), \theta_2(t))$, $\mathbf{f}_\mathscr{F}$ a source term, $\mathbf{u}^i$ a given inflow and $(.,.)_S$ the scalar product

$$(\boldsymbol{\phi},\boldsymbol{\psi})_S = \int_{S_{\rm ref}} \rho\boldsymbol{\phi}(\mathbf{y})\cdot\boldsymbol{\psi}(\mathbf{y})\,\mathrm{d}\mathbf{y}.$$

We use the notations

$$Q_\theta^\infty = \bigcup_{t\in(0,\infty)} (\{t\}\times\mathscr{F}(\theta_1(t),\theta_2(t))), \quad \Sigma_\theta^\infty = \bigcup_{t\in(0,\infty)} (\{t\}\times\partial S(\theta_1(t),\theta_2(t))),$$

$$\Sigma_i^\infty = (0,\infty)\times\Gamma_i, \quad \Sigma_w^\infty = (0,\infty)\times\Gamma_w, \quad \Sigma_N^\infty = (0,\infty)\times\Gamma_N.$$

The resulting fluid–structure system reads for $t \in (0, T)$

$$
\left\{\begin{array}{ll}
\dfrac{\partial \mathbf{u}}{\partial t}+(\mathbf{u}\cdot\nabla)\mathbf{u}-\operatorname{div}\sigma_F(\mathbf{u},p)=\mathbf{f}_{\mathscr{F}}, & \text{in } Q_\theta^\infty,\\
\operatorname{div}\mathbf{u}=0, & \text{in } Q_\theta^\infty,\\
\mathbf{u}=\dot\theta_1\partial_{\theta_1}\mathbf{X}(\theta_1,\theta_2,\mathbf{Y}(\theta_1,\theta_2,.))+\dot\theta_2\partial_{\theta_2}\mathbf{X}(\theta_1,\theta_2,\mathbf{Y}(\theta_1,\theta_2,.)), & \text{on}\,\Sigma_\theta^\infty,\\
\mathbf{u}=\mathbf{u}^i \text{ on } \Sigma_i^\infty, \quad \mathbf{u}=0 \text{ on } \Sigma_w^\infty, \quad \sigma_F(\mathbf{u},p)\mathbf{n}(.)=0 \text{ on } \Sigma_N^\infty, & \\
\mathbf{u}(0,.)=\mathbf{u}_0(.), & \text{on } \mathscr{F}(\theta_{1,0},\theta_{2,0}),\\
\mathcal{M}_{\theta_1,\theta_2}\begin{pmatrix}\ddot\theta_1\\ \ddot\theta_2\end{pmatrix}=\mathbf{M_A}(\theta_1,\theta_2,-\sigma_F(\mathbf{u},p)\mathbf{n}_{\theta_1,\theta_2})+\mathbf{M_I}(\theta_1,\theta_2,\dot\theta_1,\dot\theta_2)-k\begin{pmatrix}\theta_1\\ \theta_2\end{pmatrix}+\mathbf{h}+\mathbf{f_s}, & \\
\theta_1(0)=\theta_{1,0}, \quad \theta_2(0)=\theta_{2,0}, \ \dot\theta_1(0)=\omega_{1,0}, \quad \dot\theta_2(0)=\omega_{2,0}, \text{ where} &
\end{array}\right. \tag{1}
$$

$$
\mathcal{M}_{\theta_1,\theta_2}=\begin{pmatrix}(\partial_{\theta_1}\mathbf{X}(\theta_1,\theta_2),\partial_{\theta_1}\mathbf{X}(\theta_1,\theta_2,.))_S & (\partial_{\theta_2}\mathbf{X}(\theta_1,\theta_2),\partial_{\theta_1}\mathbf{X}(\theta_1,\theta_2,.))_S\\ (\partial_{\theta_1}\mathbf{X}(\theta_1,\theta_2),\partial_{\theta_2}\mathbf{X}(\theta_1,\theta_2,.))_S & (\partial_{\theta_2}\mathbf{X}(\theta_1,\theta_2),\partial_{\theta_2}\mathbf{X}(\theta_1,\theta_2,.))_S\end{pmatrix}\in\mathbb{R}^{2\times 2},
$$

$$
\mathbf{M_I}(\theta_1,\theta_2,\dot\theta_1,\dot\theta_2)=\begin{pmatrix}-(\dot\theta_1^2\partial_{\theta_1\theta_1}\mathbf{X}(\theta_1,\theta_2,.)+2\dot\theta_1\dot\theta_2\partial_{\theta_1\theta_2}\mathbf{X}(\theta_1,\theta_2,.)+\dot\theta_2^2\partial_{\theta_2\theta_2}\mathbf{X}(\theta_1,\theta_2),\partial_{\theta_1}\mathbf{X}(\theta_1,\theta_2,.))_S\\ -(\dot\theta_1^2\partial_{\theta_1\theta_1}\mathbf{X}(\theta_1,\theta_2,.)+2\dot\theta_1\dot\theta_2\partial_{\theta_1\theta_2}\mathbf{X}(\theta_1,\theta_2,.)+\dot\theta_2^2\partial_{\theta_2\theta_2}\mathbf{X}(\theta_1,\theta_2),\partial_{\theta_2}\mathbf{X}(\theta_1,\theta_2,.))_S\end{pmatrix}\in\mathbb{R}^2,
$$

$$
\mathbf{M_A}(\theta_1,\theta_2,-\sigma_F(\mathbf{u},p)\mathbf{n}_{\theta_1,\theta_2})=\begin{pmatrix}\displaystyle\int_{\partial S(\theta_1,\theta_2)}-\sigma_F(\mathbf{u},p)\mathbf{n}_{\theta_1,\theta_2}\cdot\partial_{\theta_1}\mathbf{X}(\theta_1,\theta_2,\mathbf{Y}(\theta_1,\theta_2,\gamma_x))\,\mathrm{d}\gamma_x\\ \displaystyle\int_{\partial S(\theta_1,\theta_2)}-\sigma_F(\mathbf{u},p)\mathbf{n}_{\theta_1,\theta_2}\cdot\partial_{\theta_2}\mathbf{X}(\theta_1,\theta_2,\mathbf{Y}(\theta_1,\theta_2,\gamma_x))\,\mathrm{d}\gamma_x\end{pmatrix}\in\mathbb{R}^2,
$$

$\mathbf{u}_0(.),\theta_{1,0},\theta_{2,0},\omega_{1,0},\omega_{2,0}$ are initial data and $\mathbf{h}\in\mathrm{L}^2(0,T;\mathbb{R}^2)$ is a control modelling a force acting on the structure, $k>0$ is a constant used to introduce a damping and $\mathbf{f_s}$ is a constant force that constraints the structure to be in a given reference position. In the sequel, we denote $\mathbf{M_I}(\theta_1,\theta_2,\dot\theta_1,\dot\theta_2)=\mathbf{M_I}(t)$ and $\mathbf{M_A}(\theta_1,\theta_2,-\sigma_F(\mathbf{u},p)\mathbf{n}_{\theta_1,\theta_2})=\mathbf{M_A}(t)$. For $T>0$ small enough, under some compatibility conditions for the initial data, there exists a strong solution to the problem (1), see [3].

2.2 The diffeomorphisms used to model the deformation of the structure given by a finite number of parameters

2.2.1 The diffeomorphism X

We consider that every fibre of matter stays normal to the mid–line in every configuration. Hence the deformation of the structure is given by the deformation of the mid–line.

The deformation of the mid–line. In the non–deformed configuration, the mid–line goes from $\ell=0$ to $\ell=1$. Let $x_a<x_b$ be in $(0,1)$, we want the mid–line to be at rest in $(0,x_a)$ and be a straight line of slope θ_2 (the first parameter to characterize the structure) in $(x_b,1)$ and we consider on (x_a,x_b) the parabola

$$
f(x)=\frac{\tan(\theta_2/2)}{x_b-x_a}(x-x_c)^2-\tan(\theta_2/2)\frac{x_b-x_a}{4}, \quad \text{with} \quad x_c=(x_a+x_b)/2,
$$

such that we have a $\mathscr{C}^1$ curve on $[0,1]$, see Fig.2(a). The next step is to rotate this parabola around $(x_a,0)$ with an angle $\theta_2/2$, to prolong it on the left hand-side by $y=0$ and on the right by a straight line of slope θ_2. This will give the desired deformation for the mid–line, see Fig.2(b), the point $B'=(x_{B'},y_{B'})^T=(x_a+(x_b-x_a)\cos(\theta_2/2),(x_b-x_a)\sin(\theta_2/2))^T$. The mid–line is then given by the parametric representation $\ell\to(g_x(\ell),g_y(\ell))^T$ where

$$
g_x(\ell)=\begin{cases}\ell & \\ x_a+(\ell-x_a)\cos(\frac{\theta_2}{2})-f(\ell)\sin(\frac{\theta_2}{2}) & \\ x_{B'}+(\ell-x_b)\cos\theta_2 & \end{cases}
\quad
g_y(\ell)=\begin{cases}0 & \text{if } \ell\le x_a,\\ (\ell-x_a)\sin(\frac{\theta_2}{2})+f(\ell)\cos(\frac{\theta_2}{2}) & \text{if } \ell\in(x_a,x_b),\\ y_{B'}+(\ell-x_b)\sin\theta_2 & \text{if } \ell\ge x_b.\end{cases}
$$

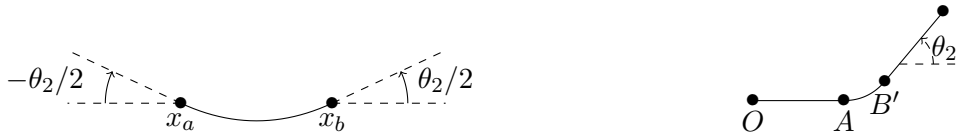

Figure 2: (a) The parabola $f(x)$, (b) the deformation of the mid–line.

Deformation of the structure. In the sequel, $\mathbf{y} = (y_1, y_2)$ denotes the Lagrangian coordinates and $\mathbf{N}(\ell) = \begin{pmatrix} N_x(\ell) \\ N_y(\ell) \end{pmatrix} = \begin{pmatrix} -g_x'(\ell) \\ g_y'(\ell) \end{pmatrix}$ is normal to the mid–line. We define the following diffeomorphism $\tilde{\mathbf{X}}(\theta_2, \mathbf{y}) = \left(g_x(y_1) + y_2 \frac{N_x(y_1)}{|\mathbf{N}(y_1)|}, g_y(y_1) + y_2 \frac{N_y(y_1)}{|\mathbf{N}(y_1)|} \right)^T$.

The rotation of the deformed structure. We get the final diffeomorphism $\mathbf{X}$ after a rotation R_{θ_1} of angle θ_1 (the second parameter to characterize the structure) around the center O, see Fig. 3, $\mathbf{X}(\theta_1, \theta_2, \mathbf{y}) = R_{\theta_1} \tilde{\mathbf{X}}(\theta_2, \mathbf{y})$ where $\mathrm{R}_{\theta_1} = \begin{pmatrix} \cos\theta_1 & -\sin\theta_1 \\ \sin\theta_1 & \cos\theta_1 \end{pmatrix}$.

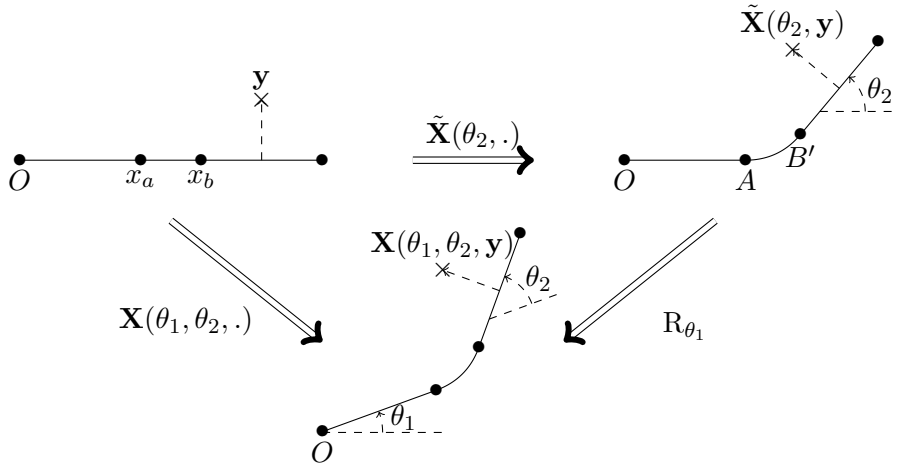

Figure 3: The diffeomorphisms $\mathbf{X}$ and $\tilde{\mathbf{X}}$.

Deformation of the profile's boundary. We consider a reference configuration for the structure $S_{\mathrm{ref}} = S(0,0)$. The boundary of this structure is described by two parametric functions: $\boldsymbol{\gamma}^+(\ell)$ for the extrados and $\boldsymbol{\gamma}^-(\ell)$ for the intrados. The boundary of $S(\theta_1(t), \theta_2(t))$ is then described by the two parametric functions $\mathbf{X}(\theta_1, \theta_2, \boldsymbol{\gamma}^+(\ell))$ and $\mathbf{X}(\theta_1, \theta_2, \boldsymbol{\gamma}^-(\ell))$, where

$$\mathbf{X}(\theta_1, \theta_2, \boldsymbol{\gamma}^+(\ell)) = \begin{pmatrix} \cos\theta_1 & -\sin\theta_1 \\ \sin\theta_1 & \cos\theta_1 \end{pmatrix} \begin{pmatrix} g_x(\gamma_x^+(\ell)) + \gamma_y^+(\ell) \frac{N_x(\gamma_x^+(\ell))}{|\mathbf{N}(\gamma_x^+(\ell))|} \\ g_y(\gamma_x^+(\ell)) + \gamma_y^+(\ell) \frac{N_y(\gamma_x^+(\ell))}{|\mathbf{N}(\gamma_x^+(\ell))|} \end{pmatrix}, \quad (2)$$

and the expression of $\mathbf{X}(\theta_1, \theta_2, \boldsymbol{\gamma}^-(\ell))$ is the analogy. In the sequel, for numerical tests, we consider the case of an elliptic symmetric reference domain, see Fig.4.
Its boundary is given by the functions

$$\begin{cases} \boldsymbol{\gamma}^+(\ell) = (\ell, \gamma_2^+(\ell)), \\ \boldsymbol{\gamma}^-(\ell) = (\ell, -\gamma_2^+(\ell)), \end{cases} \quad \text{where} \quad \gamma_2^+(\ell) = \begin{cases} b\sqrt{1 - \left(\frac{\ell - x_a}{x_a}\right)^2} & \text{if } \ell \in [0, x_a], \\ b\sqrt{1 - \left(\frac{\ell - x_a}{1 - x_a}\right)^2} & \text{if } \ell \in]x_a, 1]. \end{cases} \quad (3)$$

This explicit expression allows us to construct a set of ordered points to describe the structure's profile.

Remark 2.1. The framework presented can be used for more general geometries.

2.2.2 The diffeomorphism $\mathbf{\Phi}$

We consider a stationary configuration $S_s = S(\eta_1, \eta_2)$. Let $\tilde{\Omega} \subset \Omega$ be a smooth domain such that for every $(\theta_1, \theta_2) \in \mathbb{D}_\Theta$, we have $S(\theta_1, \theta_2) \subset \tilde{\Omega}$. Let $(\theta_1, \theta_2) \in \mathbb{D}_\Theta$, see Fig.4 and we consider $\mathbf{s}_{\theta_1,\theta_2}$ the solution to

$$\begin{cases} \Delta \mathbf{s}_{\theta_1,\theta_2} = 0 & \text{in } \tilde{\Omega}\backslash S_s, \\ \mathbf{s}_{\theta_1,\theta_2} = \mathbf{X}(\eta_1+\theta_1, \eta_2+\theta_2, \mathbf{Y}(\eta_1,\eta_2,.)) - \mathrm{Id} & \text{on } \partial S_s, \\ \mathbf{s}_{\theta_1,\theta_2} = 0 & \text{on } \partial\tilde{\Omega}. \end{cases} \tag{4}$$

We define the diffeomorphism $\mathbf{\Phi}$ by

$$\forall (\theta_1,\theta_2) \in \mathbb{D}_\Theta, \forall \mathbf{y} \in \Omega, \mathbf{\Phi}(\theta_1,\theta_2,\mathbf{y}) = \begin{cases} \mathbf{X}(\eta_1+\theta_1, \eta_2+\theta_2, \mathbf{Y}(\eta_1,\eta_2,\mathbf{y})) & \text{if } \mathbf{y} \in S_s, \\ \mathbf{y} + \mathbf{s}_{\theta_1,\theta_2}(\mathbf{y}) & \text{if } \mathbf{y} \in \tilde{\Omega}\backslash S_s, \\ \mathbf{y} & \text{if } \mathbf{y} \in \Omega\backslash\tilde{\Omega}. \end{cases}$$

and verify that

$$\partial_{\theta_j}\mathbf{\Phi}(\theta_1,\theta_2,\mathbf{y}) = \begin{cases} \partial_{\theta_j}\mathbf{X}(\eta_1+\theta_1, \eta_2+\theta_2, \mathbf{Y}(\eta_1,\eta_2,\mathbf{y})) & \text{if } \mathbf{y} \in S_s, \quad (5) \\ \partial_{\theta_j}\mathbf{s}_{\theta_1,\theta_2}(\mathbf{y}) & \text{if } \mathbf{y} \in \tilde{\Omega}\backslash S_s, \quad (6) \\ 0 & \text{if } \mathbf{y} \in \Omega\backslash\tilde{\Omega}, \end{cases}$$

where $\partial_{\theta_j}\mathbf{s}_{\theta_1,\theta_2}$ is solution to

$$\begin{cases} \Delta(\partial_{\theta_j}\mathbf{s}_{\theta_1,\theta_2}) = 0 & \text{in } \tilde{\Omega}\backslash S_s, \\ \partial_{\theta_j}\mathbf{s}_{\theta_1,\theta_2} = \partial_{\theta_j}\mathbf{X}(\eta_1+\theta_1, \eta_2+\theta_2, \mathbf{Y}(\eta_1,\eta_2,.)) & \text{on } \partial S_s, \\ \partial_{\theta_j}\mathbf{s}_{\theta_1,\theta_2} = 0 & \text{on } \partial\tilde{\Omega}. \end{cases}$$

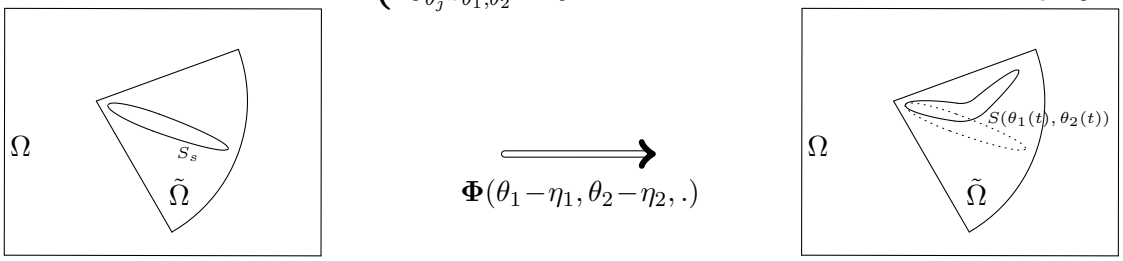

Figure 4: The diffeomorphism $\mathbf{\Phi}$.

3 Stabilization of the linear problem

In order to construct a linear feedback law that is easy to compute and able to locally stabilize the nonlinear fluid–structure problem with any exponential decay rate, we follow a strategy summarized in six following steps, we refer to [1] for more details

Step 1: We write the equations in the fixed domain $\mathscr{F}_s = \Omega\backslash S(0,0)$ using the change of variable $\mathbf{u}_{ref}(\mathbf{y}) = \mathrm{cof}(\nabla\mathbf{\Phi}(\theta_1,\theta_2,\mathbf{y}))^T\mathbf{u}_h \circ \mathbf{\Phi}(\theta_1,\theta_2,\mathbf{y})$. We linearize the resulting system around a stationary solution to the fluid–structure problem $(\mathbf{u_s}, p_s, \eta_1, \eta_2, 0, 0)^T$ and then we define the matrix formulation of the linear discretized problem with Lagrange multipliers.

Step 2: We give a reformulation of the finite dimensional linear system after elimination of the Lagrange multipliers from the equations by using a projector which plays a similar role to the Leray projector (for the infinite dimensional system).

Step 3: The construction of the linear feedback law based on previous steps is numerically difficult to compute. To overcome this difficulty we study the relationships between the eigenvalue problems (initial problem and projected problem).

Step 4: We define the projected systems associated to the unstable part of the spectral decomposition. Stabilization of the unstable part is sufficient to stabilize the whole system.

Step 5: We define the linear feedback law $\mathbf{h}$ by solving an Algebraic Riccati Equation of small dimension (Optimal control problem on Reduced Order Model).

Step 6: We stabilize the nonlinear system using $\mathbf{h}$ defined on the linear system.

At the end of the process, we have constructed the matrix $\mathbf{K}$ such that the feedback law $\mathbf{h}$ is given by the relation

$$\mathbf{h} = \mathbf{K}(\mathbf{z} - \mathbf{z_s}) \tag{7}$$

where $\mathbf{z} = (\mathbf{u}_{ref}, \theta_1, \theta_2, \omega_1, \omega_2)^T$ and $\mathbf{z_s} = (\mathbf{u_s}, \eta_1, \eta_2, 0, 0)^T$. Note that the feedback is defined in a fixed reference configuration $\mathscr{F}_s$, so $\mathbf{z}$ must be known on $\mathscr{F}_s$ at each time step.

In *Step 1*, writing the equations in the fixed domain, introduces some additional nonlinear terms (geometrical terms) that must be linearized and must be taken into account in the definition of the feedback. We refer to the paper [3] for the expression of that terms. Contrary to previous works, the numerical simulations are based on fictitious domain method that does not require to consider those additional terms. In our knowledge this strategy in control theory is new and powerful.

4 The discretization and time evolution of the fluid–structure system

This section presents the approximation of the coupled problem (1). To take into account the Dirichlet boundary conditions of the fluid on Γ_D and at the interface between the fluid and the structure, we introduce $\boldsymbol{\lambda}$ a Lagrange multiplier defined by $\boldsymbol{\lambda} = (\boldsymbol{\lambda}_{\rm s}, \boldsymbol{\lambda}_{\rm i}, \boldsymbol{\lambda}_{\rm w})^T$. We introduce finite-dimensional subspaces $V_h \subset V = \mathbf{H}^1(\mathscr{F}(\theta_1, \theta_2); \mathbb{R}^2)$ for the velocity, $Q_h \subset Q = \mathrm{L}^2(\mathscr{F}(\theta_1, \theta_2))$ for the pressure, $W_h \subset W = \mathbf{H}^{-1/2}(\partial S(\theta_1, \theta_2)) \times \mathbf{H}^{-1/2}(\Gamma_{\rm D})$ for the multipliers.

$$\begin{array}{l}
\text{Find } (\theta_1, \theta_2, \omega_1, \omega_2) \in H^2(0,T;\mathbb{D}_\Theta) \times H^1(0,T;\mathbb{R}^2) \\
\text{and } (\mathbf{u}, p, \boldsymbol{\lambda}) \in H^1_{loc}((0,\infty); V_h) \times L^2_{loc}((0,\infty); Q_h) \times L^2_{loc}((0,\infty); W_h) \text{ such that} \\
\left\{ \begin{array}{l}
\displaystyle\int_{\mathscr{F}(\theta_1,\theta_2)} \frac{\partial \mathbf{u}}{\partial t} \cdot \mathbf{v} + (\mathbf{u}\cdot\nabla)\mathbf{u}\cdot\mathbf{v} + \frac{\nu}{2}(\nabla\mathbf{u} + \nabla\mathbf{u}^T) : (\nabla\mathbf{v} + \nabla\mathbf{v}^T) - p\mathrm{div}\ \mathbf{v}\ \mathrm{d}\mathbf{x} + \int_{\Gamma_{\rm D}\cup\partial S(\theta_1,\theta_2)} \boldsymbol{\lambda}\cdot\mathbf{v}\ \mathrm{d}\gamma_x = 0, \\
\displaystyle\int_{\mathscr{F}(\theta_1,\theta_2)} q\mathrm{div}\ \mathbf{u}\ \mathrm{d}\mathbf{x} = 0, \\
\displaystyle\int_{\Gamma_{\rm D}\cup\partial S(\theta_1,\theta_2)} \mathbf{u}\cdot\boldsymbol{\mu}\ \mathrm{d}\gamma_x = \int_{\Gamma_{\rm i}} \mathbf{u}^i\cdot\boldsymbol{\mu}\ \mathrm{d}\gamma_x + \int_{\partial S(\theta_1,\theta_2)} \sum_j \omega_j \partial_{\theta_j}\mathbf{X}(\theta_1,\theta_2,\mathbf{Y}(\theta_1,\theta_2,\gamma_x))\cdot\boldsymbol{\mu}\ \mathrm{d}\gamma_x,
\end{array} \right. \\
\text{for every } (\mathbf{v}, q, \boldsymbol{\mu}) \in V_h \times Q_h \times W_h \text{ and} \\
\left\{ \begin{array}{l}
\mathcal{M}_{\theta_1,\theta_2} \begin{pmatrix} \dot\omega_1 \\ \dot\omega_2 \end{pmatrix} = \left(\displaystyle\int_{\partial S(\theta_1,\theta_2)} \boldsymbol{\lambda}\cdot\partial_{\theta_j}\mathbf{X}(\theta_1,\theta_2,\mathbf{Y}(\theta_1,\theta_2,\gamma_x))\ \mathrm{d}\gamma_x \right)_{j=1,2} + \mathbf{M_I}(\theta_1,\theta_2,\omega_1,\omega_2) - k\begin{pmatrix} \theta_1 \\ \theta_2 \end{pmatrix} + \mathbf{h}, \\
\omega_1 = \dot\theta_1, \\
\omega_2 = \dot\theta_2.
\end{array} \right.
\end{array} \tag{8}$$

In what follows, Δt denotes the time-step length, $t_n = n\Delta t$ for $n \in \mathbb{N}$. First, we discuss the discretization based on a fictitious domain method for the fluid equations (Navier-Stokes) [4]. The approximation of the structure equations is realized by a backward finite difference scheme. In this section, we describe the algorithm which is of partitioned type to prescribe the time evolution. The location of the interface is governed by a level-set. Finally, we present an original treatment of the feedback that must be done into the reference configuration. Specific manipulations must be done to obtain an efficient algorithm.

4.1 Fluid approximation : Unfitted Extended Finite Element method with Lagrange multipliers

We define a background mesh covering Ω. The interface between the fluid and the solid can arbitrary cut this mesh, see for instance Fig.5 where different zones are highlighted.

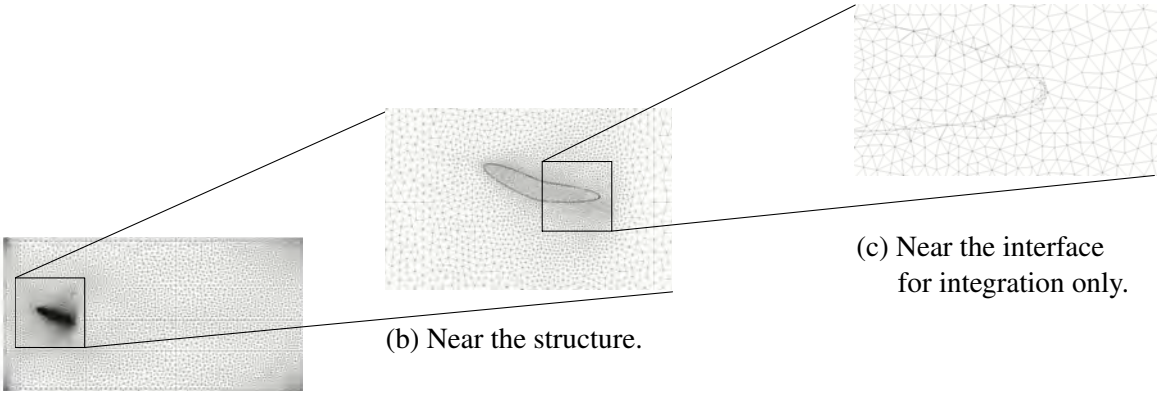

(a) Global domain.

(b) Near the structure.

(c) Near the interface for integration only.

Figure 5: The fictitious domain.

We use Lagrange multipliers to enforce the Dirichlet boundary conditions. We define a triangulation $\mathcal{T}_h$ of Ω and a background finite element method with $\mathbb{P}_2$–$\mathbb{P}_1$–$\mathbb{P}_1$ Taylor–Hood elements for the velocity, the pressure and the multipliers respectively,

$$\begin{aligned}\widetilde{V_h} &= \{\mathbf{u}_h \in \mathscr{C}^0(\Omega) \ \text{ with } \ \mathbf{u}_{h|T} \in (\mathbb{P}_2(T))^2, \quad \forall T \in \mathcal{T}_h\},\\ \widetilde{Q_h} &= \{p_h \in \mathscr{C}^0(\Omega) \ \text{ with } \ p_{h|T} \in \mathbb{P}_1(T), \quad \forall T \in \mathcal{T}_h\},\\ \widetilde{W_h} &= \{\boldsymbol{\lambda}_h \in \mathscr{C}^0(\Omega) \ \text{ with } \ \boldsymbol{\lambda}_{h|T} \in (\mathbb{P}_1(T))^2, \quad \forall T \in \mathcal{T}_h\}.\end{aligned}$$

The basis functions that are considered in the sequel are traces of the background basis functions of $\widetilde{V_h}$, $\widetilde{Q_h}$ and $\widetilde{W_h}$. The traces are taken over the fluid domain $\mathscr{F}(\theta_1, \theta_2)$ for the basis functions of the velocity and the pressure and on the interface $\partial S(\theta_1, \theta_2)$ for the Lagrange multipliers. More precisely, we consider the following natural discretizations of V, Q and W spaces,

$$V_h^n = \widetilde{V_h}_{|\mathscr{F}(\theta_1^n, \theta_2^n)}, \ \ Q_h^n = \widetilde{Q_h}_{|\mathscr{F}(\theta_1^n, \theta_2^n)}, \ \ W_h^n = \widetilde{W_h}_{|\partial S(\theta_1^n, \theta_2^n)}.$$

The fluid domain $\mathscr{F}(\theta_1^n, \theta_2^n)$ and the interface $\partial S(\theta_1^n, \theta_2^n)$ depend on the parameters of the structure (θ_1^n, θ_2^n), hence this dependence occurs also on the trace spaces. That is why we have used the superscript n on these spaces.

Similarly to XFEM, where the shape functions of the finite element space is multiplied with an Heaviside function, this corresponds here to the multiplication of the shape functions with the characteristic function of the fluid domain.

An approximation of the problem (8) can be easily given replacing the continuous functions $\mathbf{u}, p, \boldsymbol{\lambda}$ by the discrete ones $\mathbf{u}_h, p_h, \boldsymbol{\lambda}_h$. However it is known that it is not sufficient to recover the correct solution. Even if the equations are integrated only over the physical domain, to obtain stable discretizations, the approximation spaces must be carefully chosen or a stabilization term must be added to ensure an inf-sup condition. In the present work, we add the term

$$-\gamma_0 h \int_{\partial S(\theta_1,\theta_2)} (\boldsymbol{\lambda}_h + \sigma_F(\mathbf{u}_h, p_h)\mathbf{n}_{\theta_1,\theta_2}) \cdot (\boldsymbol{\mu}_h + \sigma_F(\mathbf{v}_h, q_h)\mathbf{n}_{\theta_1,\theta_2}) \, \mathrm{d}\gamma_x, \tag{9}$$

with a mesh–independent constant $\gamma_0 > 0$. It results a stable and optimally convergent approximation (in particular for the multiplier $\boldsymbol{\lambda}$) provided any mesh element T is cut by the interface in a certain way so that $\mathscr{F}(\theta_1, \theta_2) \cap T$ is a big enough portion of T. If for some elements, this is not the case, the method can be still cured by replacing the approximating polynomial in such "bad elements" by the polynomial extended from adjacent "good elements". In the stabilization term (9), the variables $\mathbf{u}$ and p are considered under this "robust reconstruction" and we specify this writing $\widehat{\mathbf{u}}$ and $\widehat{p}$ in the approximations. In practice, the assumptions required to ensure robustness of the method are satisfied if the mesh is sufficiently refined near the interface, see [4]. We denote $(\mathcal{U}_k)$, $(\mathcal{P}_k)$, $(\mathcal{W}_k)$ the basis functions of V_h^{n+1}, Q_h^{n+1}, W_h^{n+1} respectively and $\mathbf{U}$, $\mathbf{P}$, $\mathbf{\Lambda}$ are the coefficients of $\mathbf{u}_h$, p_h, $\boldsymbol{\lambda}_h$ in those basis. We realize a finite element approximation of the problem (8) where first order Euler finite difference in time is used. Note that the problem is formulated on $\mathscr{F}(\theta_1^{n+1}, \theta_2^{n+1})$ and we have to solve the following linear system for the fluid

$$(M^{n+1} + \Delta t A^{n+1})\mathbf{Z}^{n+1} = \Delta t \mathbf{F}^{n+1} + M^{n+1}\mathbf{Z}^n, \tag{10}$$

where those vectors and matrices are given by

$$M^{n+1} = \begin{pmatrix} M_{\mathbf{uu}} & 0 & 0 \\ 0 & 0 & 0 \\ 0 & 0 & 0 \end{pmatrix}, \; A^{n+1} = \begin{pmatrix} A_{\mathbf{uu}} & A_{\mathbf{u}p} & A_{\mathbf{u}\boldsymbol{\lambda}} \\ A_{\mathbf{u}p}^T & A_{pp} & A_{p\boldsymbol{\lambda}} \\ A_{\mathbf{u}\boldsymbol{\lambda}}^T & A_{p\boldsymbol{\lambda}}^T & A_{\boldsymbol{\lambda}\boldsymbol{\lambda}} \end{pmatrix}, \; \mathbf{Z} = \begin{pmatrix} \mathbf{U} \\ \mathbf{P} \\ \mathbf{\Lambda} \end{pmatrix} \text{ and } \mathbf{F} = \begin{pmatrix} 0 \\ 0 \\ F_{\boldsymbol{\lambda}} \end{pmatrix}, \text{ with}$$

$$\begin{aligned}
(M_{\mathbf{uu}})_{jk} &= \int_{\mathscr{F}(\theta_1^{n+1},\theta_2^{n+1})} \mathcal{U}_j \cdot \mathcal{U}_k \, \mathrm{d}\mathbf{x}, \qquad (A_{pp})_{jk} = -\gamma_0 h \int_{\partial S(\theta_1^{n+1},\theta_2^{n+1})} \widehat{\mathcal{P}_j}\widehat{\mathcal{P}_k} \, \mathrm{d}\gamma_x, \\
(A_{\mathbf{uu}})_{jk} &= \int_{\mathscr{F}(\theta_1^{n+1},\theta_2^{n+1})} (\mathbf{u}_h^n \cdot \nabla)\mathcal{U}_k \cdot \mathcal{U}_j + \frac{\nu}{2}(\nabla \mathcal{U}_j + \nabla \mathcal{U}_j^T) : (\nabla \mathcal{U}_k + \nabla \mathcal{U}_k^T) \, \mathrm{d}\mathbf{x} \\
&\quad -\nu^2 \gamma_0 h \int_{\partial S(\theta_1^{n+1},\theta_2^{n+1})} (\nabla \widehat{\mathcal{U}_j} + \nabla \widehat{\mathcal{U}_j}^T)\mathbf{n}_{\theta_1,\theta_2} \cdot (\nabla \widehat{\mathcal{U}_k} + \nabla \widehat{\mathcal{U}_k}^T)\mathbf{n}_{\theta_1,\theta_2} \, \mathrm{d}\gamma_x, \\
(A_{\mathbf{u}p})_{jk} &= -\int_{\mathscr{F}(\theta_1^{n+1},\theta_2^{n+1})} \mathcal{P}_k \mathrm{div}\, \mathcal{U}_j \, \mathrm{d}\mathbf{x} + \nu\gamma_0 h \int_{\partial S(\theta_1^{n+1},\theta_2^{n+1})} \widehat{\mathcal{P}_k}\mathbf{n}_{\theta_1,\theta_2} \cdot (\nabla \widehat{\mathcal{U}_j} + \nabla \widehat{\mathcal{U}_j}^T)\mathbf{n}_{\theta_1,\theta_2} \, \mathrm{d}\gamma_x, \\
(A_{\mathbf{u}\boldsymbol{\lambda}})_{jk} &= -\int_{\Gamma_{\mathrm{D}} \cup \partial S(\theta_1^{n+1},\theta_2^{n+1})} \mathcal{U}_j \cdot \mathcal{W}_k \, \mathrm{d}\gamma_x - \nu\gamma_0 h \int_{\partial S(\theta_1^{n+1},\theta_2^{n+1})} \mathcal{W}_k \cdot (\nabla \widehat{\mathcal{U}_j} + \nabla \widehat{\mathcal{U}_j}^T)\mathbf{n}_{\theta_1,\theta_2} \, \mathrm{d}\gamma_x, \\
(A_{p\boldsymbol{\lambda}})_{jk} &= \gamma_0 h \int_{\partial S(\theta_1^{n+1},\theta_2^{n+1})} \widehat{\mathcal{P}_j}\mathbf{n}_{\theta_1,\theta_2} \cdot \mathcal{W}_k \, \mathrm{d}\gamma_x, \qquad (A_{\boldsymbol{\lambda}\boldsymbol{\lambda}})_{jk} = -\gamma_0 h \int_{\partial S(\theta_1^{n+1},\theta_2^{n+1})} \mathcal{W}_j \cdot \mathcal{W}_k \, \mathrm{d}\gamma_x, \\
(F_{\boldsymbol{\lambda}})_k &= \int_{\Gamma_{\mathrm{i}}} \mathbf{u}^i \cdot \mathcal{W}_k \, \mathrm{d}\gamma_x + \int_{\partial S(\theta_1^{n+1},\theta_2^{n+1})} \sum_j \omega_j^{n+1} \partial_{\theta_j} \mathbf{X}(\theta_1^{n+1}, \theta_2^{n+1}, \mathbf{Y}(\theta_1^{n+1}, \theta_2^{n+1}, \gamma_x)) \cdot \mathcal{W}_k \, \mathrm{d}\gamma_x.
\end{aligned}$$

4.2 Structure approximation

We use a Finite Difference scheme to approximate the velocity and the displacement of the structure

$$\begin{cases}
\begin{pmatrix} \theta_1^{n+1} \\ \theta_2^{n+1} \end{pmatrix} = 2\begin{pmatrix} \theta_1^{n} \\ \theta_2^{n} \end{pmatrix} - \begin{pmatrix} \theta_1^{n-1} \\ \theta_2^{n-1} \end{pmatrix} + \Delta t^2 \mathcal{M}_{\theta_1,\theta_2}^{-1} \left(\mathbf{M}_{\mathbf{A}}(t^n) + \mathbf{M}_{\mathbf{I}}(t^n) + \mathbf{h} - k \begin{pmatrix} \theta_1^{n} \\ \theta_2^{n} \end{pmatrix} \right), \\
\begin{pmatrix} \omega_1^{n+1} \\ \omega_2^{n+1} \end{pmatrix} = \begin{pmatrix} \omega_1^{n} \\ \omega_2^{n} \end{pmatrix} + \Delta t \mathcal{M}_{\theta_1,\theta_2}^{-1} \left(\mathbf{M}_{\mathbf{A}}(t^n) + \mathbf{M}_{\mathbf{I}}(t^n) + \mathbf{h} - k \begin{pmatrix} \theta_1^{n} \\ \theta_2^{n} \end{pmatrix} \right).
\end{cases} \tag{11}$$

4.3 Coupling scheme

We use a partitioned approach, see [6, 2], which means that we treat the update with two sequential steps: a fluid step and a structure step. At each time step we do the following procedure

1. Compute $\mathbf{h}$ (if the control is applied)
2. Compute $(\theta_1^{n+1}, \theta_2^{n+1}, \omega_1^{n+1}, \omega_2^{n+1})$ with the structure step (11).
3. Update the fluid domain $\mathscr{F}(\theta_1^{n+1}, \theta_2^{n+1})$ and finite element spaces V_h^{n+1}, Q_h^{n+1}, W_h^{n+1} (new definition near the interface).
4. Assembling the matrices M^{n+1}, A^{n+1} and F^{n+1} in (10).
5. Compute $(\mathbf{u}_h^{n+1}, p_h^{n+1}, \boldsymbol{\lambda}_h^{n+1})$ with the fluid step (10).
6. Compute the next time step Δt such that only one row of elements can be crossed by the structure, i.e. $\Delta t = cfl \times \dfrac{h}{V_{\max}}$, where h is the characteristic mesh-size, $V_{\max}$ is the maximum velocity of the structure and $cfl \in (0, 1)$.

4.4 Fictitious points and level-set update

During the time-marching procedure, difficulties arise near the interface. Indeed, the field variable at the time level t^{n+1} can become undefined near the interface since there was no fluid flow at the time level t^n ($S(\theta_1^{n+1}, \theta_2^{n+1}) \neq S(\theta_1^n, \theta_2^n)$ for the solid and $\mathscr{F}(\theta_1^{n+1}, \theta_2^{n+1}) \neq \mathscr{F}(\theta_1^n, \theta_2^n)$ for the fluid). In other words, some degrees of freedom for the fluid part which are not considered at the time level t^n must be taken into account at the time level t^{n+1}.

Level–set function and integration method over the cut elements. The matrices in (10) are computed via an integration over $\mathscr{F}(\theta_1, \theta_2)$ and $\partial S(\theta_1, \theta_2)$. These integration methods need a well–defined interface $\partial S(\theta_1, \theta_2)$ and a method to integrate functions over the cut elements. The interface is defined as the null level of a level–set function and the integration over the cut cells is done by dividing those cells into sub–cells, see Fig.5(c), (QHULL library). Note that the level–set is defined by a set of discrete ordered points located on the position of the interface which is known explicitly according to the parameters θ_1, θ_2 and the diffeomorphism $\mathbf{X}$, see (2). The distance to the level–set is computed by searching the two points that minimize the distance and by taking the projection on the segment defined by those two points. In order to reduce the computational cost of this method, at each time step, we compute the distance to the level–set only for the mesh nodes that are needed, i.e. the nodes near the interface. This drastically reduces the computational cost.

Treatment of the fictitious points. When solving (10) we need $\mathbf{U}^n$, the coordinates of $\mathbf{u}_h^n$ in the basis of the space V_h^{n+1} while it is known in V_h^n. Even if the computation is realized only on the fluid domain, we affect values for the velocity in each degree of freedom of the background mesh. In the fluid domain, the values come from the resolution of the Navier-Stokes equations at the time level t^n while the values in the structure come from the velocity of the structure

$$\boldsymbol{u}_{str}^n(\mathbf{x}) = \omega_1^n \partial_{\theta_1} \mathbf{X}(\theta_1^n, \theta_2^n, \mathbf{Y}(\theta_1^n, \theta_2^n, \mathbf{x})) + \omega_2^n \partial_{\theta_2} \mathbf{X}(\theta_1^n, \theta_2^n, \mathbf{Y}(\theta_1^n, \theta_2^n, \mathbf{x})).$$

In practice, for each nodes $\mathbf{y}_i$ of the mesh in the reference configuration S_{ref}, we compute $\mathbf{x}_i = \mathbf{X}(\theta_1^n, \theta_2^n, \mathbf{y}_i)$ and $\partial_{\theta_j} \mathbf{X}(\theta_1^n, \theta_2^n, \mathbf{y}_i)$ to determine the velocity $\boldsymbol{u}_{str}^n(\mathbf{x}_i)$. Considering this set of velocity values we can approximate $\boldsymbol{u}_{str}^n(\mathbf{x})$ in any point $\mathbf{x}$ (using a weighted arithmetic mean). Indeed, we do not have any explicit expression for $\mathbf{Y}(\theta_1, \theta_2, \mathbf{x})$.

Remark 4.1. For efficiency, the node $\mathbf{y}_i$ retained to compute $\boldsymbol{u}_{str}^n(\mathbf{x})$ are reduced to the ones located near the structure's boundary in S_{ref}.

4.5 Computation of the feedback control in the actual domain

The main originality of our work compared with other stabilization studies is that the simulation is run in the actual domain $\mathscr{F}(\theta_1, \theta_2)$ instead of the reference domain $\mathscr{F}_s$ corresponding to the configuration of the stationary solution. However, the feedback matrix $\mathbf{K}$ has been computed in $\mathscr{F}_s$ (see Section 3), then to apply the feedback control (7) given by $\mathbf{h} = \mathbf{K}(\mathbf{z} - \mathbf{z_s})$, we need the value of the velocity $\mathbf{u}_{ref}$ at any time iteration in the reference configuration $\mathscr{F}_s$. In order to get the value of $\mathbf{u}_{ref}$, for every node $\mathbf{y}$ of the mesh on $\mathscr{F}_s$, we use the relation

$$\mathbf{u}_{ref}(\mathbf{y}) = \mathrm{cof}(\nabla \mathbf{\Phi}(\theta_1, \theta_2, \mathbf{y}))^T \mathbf{u}_h \circ \mathbf{\Phi}(\theta_1, \theta_2, \mathbf{y}).$$

For each node $\mathbf{y}$, we compute the corresponding point $\mathbf{x} = \mathbf{\Phi}(\theta_1, \theta_2, \mathbf{y})$ in the computational domain $\mathscr{F}(\theta_1, \theta_2)$. Then we obtain the value of $\mathbf{u}_h(\mathbf{x})$ by interpolation using the velocity computed on $\mathscr{F}(\theta_1, \theta_2)$ at each time step. We can conclude by multiplying by the transposed cofactor of the Jacobian matrix of $\mathbf{\Phi}$ given by (6).

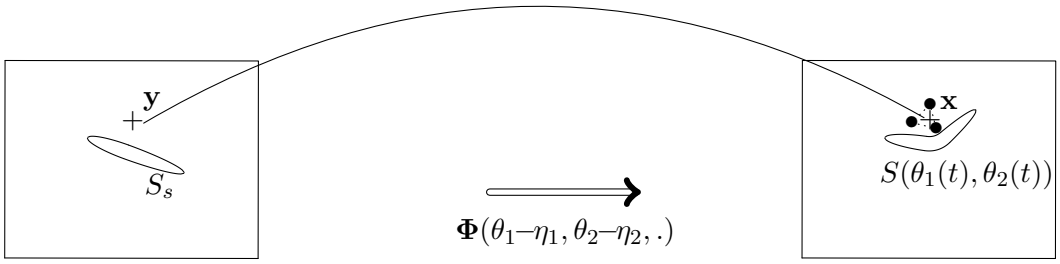

Figure 6: Interpolation to compute the velocity in the fixed domain.

To sum up, the feedback is simply based on $\mathbf{\Phi}$ numerically defined as an extension of $\mathbf{X}$ into the fluid domain and that can be obtained by solving a Poisson problem formulated on a small domain defined around the structure (see the sector in Fig.4).

5 Numerical results

We consider the configuration illustrated in Fig.1 with $\Omega = (-1.0, 8.0) \times (y_{\min}, y_{\max})$ where $y_{\min} = -2.4$, $y_{\max} = 2.1$ and the structure domain is given by (3) with the point O located in $(0, 0)$. The initial position of the structure is $(\eta_1, \eta_2) = (-25°, 0)$, the initial inflow boundary datum is given by a Poiseuille profile $\mathbf{u}^i(x_2) = \frac{6U_{\mathrm{m}}}{(y_{\max} - y_{\min})^2}(-x_2^2 + (y_{\max} + y_{\min})x_2 - y_{\max}y_{\min})$, where U_{m} is the mean speed of the inflow datum. The Reynolds number $\mathcal{R}e = \frac{cU_{\mathrm{m}}}{\nu}$, where $c = 1$ is the chord of the profile, is taken as $\mathcal{R}e = 300$. In the sequel, we use $U_{\mathrm{m}} = 1$ and $\nu = \frac{1}{300}$. The initial state of the fluid is computed as the stationary state associated to the datum $\mathbf{u}^i$. We consider on Γ_i an inflow boundary perturbation $\mathbf{u}(\mathbf{x}) = \mathbf{u}^i + \beta_p g(\mathbf{x}) e^{-30(t-0.3)^2}$, where $\beta_p > 0$ is a coefficient that represents the intensity of the perturbation (here we take $\beta_p = 0.5$), $g(\mathbf{x}) = (\sigma(\psi^1, p^1)\mathbf{n}.\mathbf{n}, 0)^T$ for ψ^1 and p^1 computed as the real part of an eigenvector associated to the most unstable eigenvalue of the adjoint problem introduced to define $\mathbf{K}_\delta$ (the vector $\sigma(\psi^1, p^1)\mathbf{n}$ was normalized). Such perturbation is one of the most destabilizing normal boundary perturbations for the fluid [1]. The parameters of the structure are given by $\rho = 5$ and $k = 12$.
The numerical computations are led on a triangular mesh of 35731 cells locally refined near the boundary, near the structure and near the wake of the structure (see Fig.5(a)). We use the finite element spaces and the time stepping process defined above. The total number of degrees of freedom is equal to 153880 at the initial time and varies according to the number of elements that are discarded.

Figure 7: (a) Spectrum of the linearized problem, (b) Inflow perturbation $\sigma(\psi^1, p^1)\mathbf{n}.\mathbf{n}$.

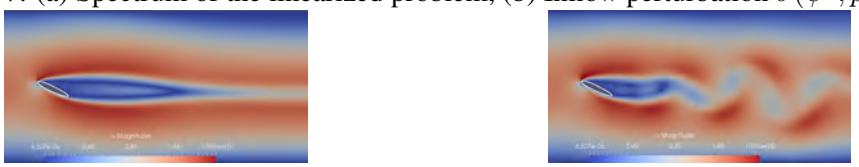

Figure 8: (a) Stationary solution (t=0s), (b) perturbated solution (t=12s) for $Re = 300$.

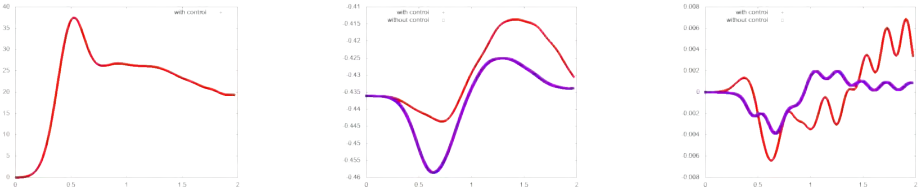

Figure 9: (a) Evolution of $\|\mathbf{u} - \mathbf{u_s}\|_2$ and (b) Evolution of θ_1 and (c) θ_2 with and without control.

We run two simulations, one in open loop and the other one in closed loop. In that way, we can observe the efficiency of the feedback control. The results are shown in Fig.9 and confirm the good behavior of the method.

References

[1] C. Airiau, J.-M. Buchot, R.K. Dubey, M. Fournié, J.-P. Raymond, and J. Weller-Carlo. Stabilization and best actuator location for the Navier–Stokes equations. *SIAM J. Sc. Comput.*, 39(5):B993–B1020, 2017.

[2] E. Burman and M.A. Fernández. An unfitted Nitsche method for incompressible fluid-structure interaction using overlapping meshes. *Comput. Methods Appl. Mech. Engrg.*, 279:497–514, 2014.

[3] G. Delay. Etude d'un problème d'interaction fluide–structure: Modélisation, Analyse, Stabilisation et Simulation numérique. *PhD thesis, Univ. de Toulouse*, 2018.

[4] M. Fournié and A. Lozinski. Stability and optimal convergence of unfitted extended finite element methods with Lagrange multipliers for the Stokes equations. *Lecture Notes in Computational Science and Engineering*, 121:143–182, 2018.

[5] M. Fournié and J. Morrison. Fictitious domain for stabilization of fluid–structure interaction. *IFAC PapersOnLine*, 50-1:12301–12306, 2017.

[6] M. Fernández and J. Mullaert. Convergence and error analysis for a class of splitting schemes in incompressible fluid–structure interaction. *IMA J. Numer. Anal.*, 36(4):1748–1782, 2016.

[7] J.C. Gomez and E. Garcia. Morphing unmanned aerial vehicles. *Smart Mater. Struct.*, 20:103001–1030171, 2011.

[8] M. Heinkenschloss, D.C. Sorensen, and K. Sun. Balanced truncation model reduction for a class of descriptor systems with application to the Oseen equations. *SIAM J. Sci. Comput.*, 30(2):1038–1063, 2008.

[9] G. Hou, J. Wang, and A. Layton. Numerical methods for fluid–structure interaction. a review. *Commun. Comput. Phys.*, 4:609–644, 2012.

[10] M. Ndiaye. Stabilisation et simulation de modèles d'interaction fluide–structure. *PhD thesis, Université de Toulouse*, 2016.